

Thin accretion disk around a rotating Kerr-like black hole in Einstein-bumblebee gravity model

Changqing Liu^{1,*}, Chikun Ding^{1,2,†} and Jiliang Jing^{2‡}

¹*Department of Physics, Hunan University of Humanities,
Science and Technology, Loudi, Hunan 417000, P. R. China*

²*Key Laboratory of Low Dimensional Quantum Structures and Quantum Control of Ministry of Education,
and Synergetic Innovation Center for Quantum Effects and Applications,
Hunan Normal University, Changsha, Hunan 410081, P. R. China*

Abstract

We study the accretion process in the thin disk around a rotating Kerr-like black hole in Einstein-bumblebee gravity model where Lorentz symmetry is spontaneously broken once a vector field acquires a vacuum expectation value. In the present paper we obtain the energy flux, the emission spectrum and accretion efficiency from the accretion disks around the rotating Kerr-like black hole, and we compare them to the general Kerr case. These significant features in the mass accretion process may provide a possibility to test whether the Lorentz symmetry is spontaneously broken or not in the Einstein-bumblebee gravity model by future astronomical observations.

PACS numbers: 04.70.Dy, 95.30.Sf, 97.60.Lf

*Electronic address: lcqliu2562@163.com

†Electronic address: Chikun.Ding@huhst.edu.cn

‡Electronic address: jljing@hunnu.edu.cn

I. INTRODUCTION

General relativity (GR) describes gravitation at a classical level. Standard Model (SM) describes particles and the other three fundamental interactions at a quantum level. In the past decades, there were some attempts to construct a fundamental theory that unifies between GR and SM theories. The unification between these two theories imply that small Lorentz violation (LV) [1, 2] effects may appear at the Planck scale and Lorentz symmetry breaking arises in the context of string theory [1], noncommutative field theories [3] or loop quantum gravity theory [4]. Some novel hypothetical effects that break local Lorentz symmetry and CPT symmetry in gravitational experiments as well as solar system and astrophysical observations have been studied in recent works. Much of this work uses the effective field theory framework. Thus, the study of Lorentz violation is a valuable tool to probe the foundations of modern physics. These studies include LV in the neutrino sector [5], the standard-model extension (SME) [6], LV in the non-gravity sector [7], and LV effect on the formation of atmospheric showers [8].

The SME is an effective field theory describing the SM coupled to GR, allowing for dynamical curvature modes, and includes additional terms containing information about the LV occurring at the Plank scale. The LV terms in the SME take the form of Lorentz-violating operators coupled to coefficients with Lorentz indices. The presence of LV in a local Lorentz frame is signaled by a nonzero vacuum value for one or more quantities carrying local Lorentz indices. The so-called bumblebee model, as one kind of the SME in the effective field theory, was first used by Kostelecky and Samuel in 1989 [1]. It is a simple model for investigating the consequences of spontaneous LV. The LV arises from the dynamics of a single vector or axial-vector field B_μ , known as the bumblebee field. It is ruled by a potential exhibiting a minimum rolls to its vacuum expectation value. Several applications with the bumblebee model have been done, such as, traversable wormhole solution in the framework of the bumblebee gravity theory [9], exact Schwarzschild-like solution [10], cosmological implications of Bumblebee vector models [11, 12], Gödel solution [13], quantum effects [14, 15]. Recently, we obtain an exact Kerr-like black hole solution [16] by solving the corresponding gravitational field equations in Einstein-bumblebee gravity model where Lorentz symmetry is spontaneously broken once a vector field acquires a vacuum expectation value.

Accretion disks are well known observationally, representing flattened astronomical structures. The accretion processes is a powerful indicator of the physical nature of the central celestial objects, which means that the analysis of the signatures of the accretion disk around the rotating Kerr like black hole could help us to

detect the Lorentz breaking effects in Einstein-bumblebee gravity model. The steady-state thin accretion disk model is the simplest theoretical model of the accretion disks, in which the disk has negligible thickness so that the heat generated by stress and dynamic friction in the disk can be dispersed through the radiation over its surface [17–21]. This cooling mechanism ensures that the disk can be in hydrodynamical equilibrium and the mass accretion rate in the disk maintains a constant, which is independent of time variable. The physical properties of matter forming a thin accretion disk in a variety of background spacetimes have been investigated extensively in [22–34]. The special signatures appeared in the energy flux and the emission spectrum emitted by the disk can provide us not only the information about black holes in the Universe, but also the profound verification of alternative theories of gravity. Therefore, in this paper, we shall focus on the influence of the Lorentz breaking parameter on the properties of the thin accretion disk around a Kerr like black hole.

The rest of the paper is organized as follows: in section II, we will review briefly the rotating Kerr like black hole metric in Einstein-bumblebee gravity model, and then present the geodesic equations for the timelike particles moving in the equatorial plane in this background. In Sec.III, we study the physical properties of the thin accretion disk around the rotating Kerr like black hole and probe the effects of the Lorentz breaking parameter on the energy flux, temperature and emission spectrum of the thin accretion disks onto this black hole. Sec. IV is devoted to a summary.

II. THE GEODESIC EQUATIONS IN THE ROTATING KERR-LIKE BLACK HOLE

Let us now review briefly the exact Kerr-like black hole [16] In the bumblebee gravity theory, the bumblebee vector field B_μ acquires a nonzero vacuum expectation value, under a suitable potential, inducing a spontaneous Lorentz symmetry breaking in the gravitational sector. It is described by the action,

$$\mathcal{S} = \int d^4x \sqrt{-g} \left[\frac{1}{16\pi G_N} (\mathcal{R} + \varrho B^\mu B^\nu \mathcal{R}_{\mu\nu}) - \frac{1}{4} B^{\mu\nu} B_{\mu\nu} - V(B^\mu B_\mu \pm b^2) \right], \quad (1)$$

where ϱ is a real coupling constant (with mass dimension -1) which controls the non-minimal gravity interaction to bumblebee field B_μ (with the mass dimension 1), and b^2 is a real positive constant. The bumblebee field strength is defined by

$$B_{\mu\nu} = \partial_\mu B_\nu - \partial_\nu B_\mu. \quad (2)$$

The potential V , driving Lorentz and/or CPT (charge, parity and time), have a minimum at $B^\mu B_\mu \pm b^2 = 0$ and $V'(b_\mu b^\mu) = 0$, where $b^\mu = \langle B^\mu \rangle$ and has constant magnitude $b_\mu b^\mu = \mp b^2$.

The action (1) yields the gravitational field equation in vacuum

$$\mathcal{R}_{\mu\nu} = \kappa T_{\mu\nu}^B + 2\kappa g_{\mu\nu}V + \frac{1}{2}\kappa g_{\mu\nu}B^{\alpha\beta}B_{\alpha\beta} - \kappa g_{\mu\nu}B^\alpha B_\alpha V' + \frac{\varrho}{4}g_{\mu\nu}\nabla^2(B^\alpha B_\alpha) + \frac{\varrho}{2}g_{\mu\nu}\nabla_\alpha\nabla_\beta(B^\alpha B^\beta), \quad (3)$$

where $\kappa = 8\pi G_N$ and the bumblebee energy momentum tensor $T_{\mu\nu}^B$ is

$$\begin{aligned} T_{\mu\nu}^B = & -B_{\mu\alpha}B_\nu^\alpha - \frac{1}{4}g_{\mu\nu}B^{\alpha\beta}B_{\alpha\beta} - g_{\mu\nu}V + 2B_\mu B_\nu V' \\ & + \frac{\varrho}{\kappa}\left[\frac{1}{2}g_{\mu\nu}B^\alpha B^\beta R_{\alpha\beta} - B_\mu B^\alpha R_{\alpha\nu} - B_\nu B^\alpha R_{\alpha\mu} \right. \\ & \left. + \frac{1}{2}\nabla_\alpha\nabla_\mu(B^\alpha B_\nu) + \frac{1}{2}\nabla_\alpha\nabla_\nu(B^\alpha B_\mu) - \frac{1}{2}\nabla^2(B^\mu B_\nu) - \frac{1}{2}g_{\mu\nu}\nabla_\alpha\nabla_\beta(B^\alpha B^\beta)\right]. \end{aligned} \quad (4)$$

The bumblebee field is fixed to be

$$B_\mu = b_\mu, \quad (5)$$

and $V = 0$, $V' = 0$. Then Eq. (3) leads to gravitational field equations

$$\bar{R}_{\mu\nu} = 0, \quad (6)$$

with

$$\begin{aligned} \bar{R}_{\mu\nu} = & \mathcal{R}_{\mu\nu} + \kappa b_{\mu\alpha}b_\nu^\alpha - \frac{\kappa}{4}g_{\mu\nu}b^{\alpha\beta}b_{\alpha\beta} + \varrho b_\mu b^\alpha \mathcal{R}_{\alpha\nu} + \varrho b_\nu b^\alpha \mathcal{R}_{\alpha\mu} - \frac{\varrho}{2}g_{\mu\nu}b^\alpha b^\beta \mathcal{R}_{\alpha\beta} + \bar{B}_{\mu\nu}, \\ \bar{B}_{\mu\nu} = & -\frac{\varrho}{2}\left[\nabla_\alpha\nabla_\mu(b^\alpha b_\nu) + \nabla_\alpha\nabla_\nu(b^\alpha b_\mu) - \nabla^2(b_\mu b_\nu)\right]. \end{aligned} \quad (7)$$

In the standard Boyer-Lindquist coordinates, the metric of this rotating Kerr-like black hole has a form [16]

$$ds^2 = g_{tt}dt^2 + g_{rr}dr^2 + g_{\theta\theta}d\theta^2 + g_{\phi\phi}d\phi^2 + 2g_{t\phi}dtd\phi, \quad (8)$$

where

$$\begin{aligned} g_{tt} &= -\left(1 - \frac{2Mr}{\rho^2}\right), \quad g_{t\phi} = -\frac{2Mr a \sqrt{1+l} \sin^2 \theta}{\rho^2}, \\ g_{rr} &= \frac{\rho^2}{\Delta}, \quad g_{\theta\theta} = \rho^2, \quad g_{\phi\phi} = \frac{A \sin^2 \theta}{\rho^2}, \end{aligned} \quad (9)$$

with

$$\rho^2 = r^2 + (1+l)a^2 \cos^2 \theta, \quad \Delta = \frac{r^2 - 2Mr}{1+l} + a^2, \quad A = [r^2 + (1+l)a^2]^2 - \Delta(1+l)a^2 \sin^2 \theta. \quad (10)$$

Here l is the LV parameter. As $l = 0$, the black hole is reduced to the usual Kerr black hole in general relativity. The metric (8) represents a purely radial Lorentz-violating black hole solution with rotating angular momentum a . It is singular at $\rho^2 = 0$ and at $\Delta = 0$. The solution of $\rho^2 = 0$ is a ring shape physical singularity

at the equatorial plane of the center of rotating black hole with radius a . Its event horizons and ergosphere locate at

$$r_{\pm} = M \pm \sqrt{M^2 - a^2(1+l)}, \quad r_{\pm}^{ergo} = M \pm \sqrt{M^2 - a^2(1+l)\cos^2\theta}, \quad (11)$$

where \pm signs correspond to outer and inner horizon/ergosphere, respectively. It is easy to see that there exists a black hole if and only if

$$|a| \leq \frac{M}{\sqrt{1+l}}. \quad (12)$$

According to the thin accretion disk model, one can assume that the disk is on the equatorial plane and that the matter moves on nearly geodesic circular orbits. In the rotating Kerr-like black hole spacetime (8), the time-like geodesics equations of a particle can be expressed as

$$u^t = \frac{dt}{d\lambda} = \frac{\tilde{E}g_{\phi\phi} - \tilde{L}g_{t\phi}}{g_{t\phi}^2 - g_{tt}g_{\phi\phi}}, \quad (13)$$

$$u^{\phi} = \frac{d\phi}{d\lambda} = \frac{\tilde{E}g_{t\phi} + \tilde{L}g_{tt}}{g_{t\phi}^2 - g_{tt}g_{\phi\phi}}, \quad (14)$$

$$g_{rr}\left(\frac{dr}{d\lambda}\right)^2 + g_{\theta\theta}\left(\frac{d\theta}{d\lambda}\right)^2 = V_{eff}, \quad (15)$$

with the effective potential

$$V_{eff} = \frac{\tilde{E}^2 g_{\phi\phi} + 2\tilde{E}\tilde{L}g_{t\phi} + \tilde{L}^2 g_{tt}}{g_{t\phi}^2 - g_{tt}g_{\phi\phi}} - 1, \quad (16)$$

where \tilde{E} and \tilde{L} are the specific energy and the specific angular momentum of the particle, respectively.

The circular equatorial orbits obey the conditions $V_{eff} = 0$, $V_{eff,r} = 0$ and $V_{eff,\theta} = 0$ [22, 23, 33]. Due to the reflection symmetry of the metric (8) with respect to the equatorial plane, one can find that the condition $V_{eff,\theta} = 0$ is satisfied naturally for the particles locating at the plane $\theta = \pi/2$. Making use of these conditions, we can get the specific energy \tilde{E} , the specific angular momentum \tilde{L} and the angular velocity Ω of the particle moving in circular orbit on the equatorial plane in the rotating Kerr-like black hole spacetime

$$\tilde{E} = -\frac{g_{tt} + g_{t\phi}\Omega}{\sqrt{-g_{tt} - 2g_{t\phi}\Omega - g_{\phi\phi}\Omega^2}} = \frac{a\sqrt{(l+1)M} + \sqrt{r}(r-2M)}{\sqrt{2ar^{3/2}\sqrt{(l+1)M} - 3Mr^2 + r^3}}, \quad (17)$$

$$\tilde{L} = \frac{g_{t\phi} + g_{\phi\phi}\Omega}{\sqrt{-g_{tt} - 2g_{t\phi}\Omega - g_{\phi\phi}\Omega^2}} = \frac{\sqrt{M}\left(a\left(a(1+l) - 2\sqrt{(l+1)Mr}\right) + r^2\right)}{\sqrt{2ar^{3/2}\sqrt{(l+1)M} - 3Mr^2 + r^3}}, \quad (18)$$

$$\Omega = \frac{d\phi}{dt} = \frac{-g_{t\phi,r} + \sqrt{g_{t\phi,r}^2 - g_{tt,r}g_{\phi\phi,r}}}{g_{\phi\phi,r}} = \frac{1}{\frac{r^{3/2}}{\sqrt{M}} + a\sqrt{1+l}}. \quad (19)$$

The marginally stable orbit radius is determined by the condition $V_{eff} = 0$, $V_{eff,r} = 0$ and $V_{eff,rr} = 0$. In fact, we can also use the conditions $d\tilde{E}/dr$ or $d\tilde{L}/dr$ [19] to obtain it. With the help of the equation (17), the marginally stable orbit on the equatorial plane is given by the following equations

$$r(r - 6M) + 8a\sqrt{Mr(1+l)} - 3a^2(1+l) = 0 \quad (20)$$

$$(21)$$

which give the radius of the marginally stable orbit as

$$r_{ms} = M \left(3 + B - \sqrt{(3-A)(3+A+2B)} \right), \quad (22)$$

$$A = \sqrt[3]{1 - \frac{a^2(l+1)}{M^2}} \left(\sqrt[3]{1 - \frac{a\sqrt{l+1}}{M}} + \sqrt[3]{\frac{a\sqrt{l+1}}{M} + 1} \right) + 1,$$

$$B = \sqrt{\frac{3a^2(l+1)}{M^2} + A^2}.$$

$$(23)$$

For $a = 0$, the marginally stable orbit radius r_{ms} is always equals to $6M$ and independent of the LV parameter l . In Fig.(1), we plot the variety of the marginally stable orbit radius r_{ms} with the LV parameter l in the rotating Kerr-like black hole. It shows that the r_{ms} decreases with l in the prograde orbit ($a > 0$), and increases with l in the retrograde orbit ($a < 0$).

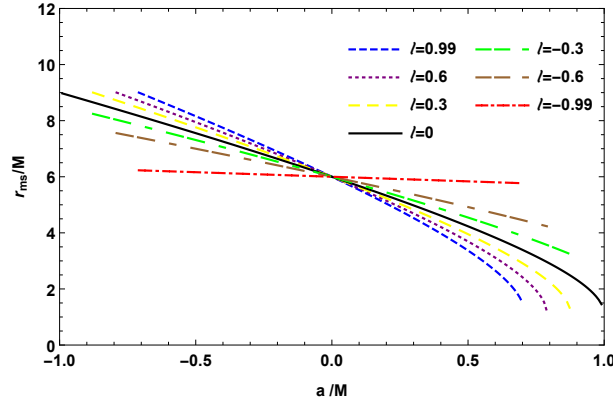


FIG. 1: The marginally stable orbit radius r_{ms} with the LV parameter l for the thin disk around the rotating Kerr-like black hole.

III. THE PROPERTIES OF THIN ACCRETION DISKS IN THE ROTATING KERR-LIKE BLACK HOLE SPACETIME

In this section we will adopt the steady-state thin accretion disk model to study the accretion process in the thin disk around the rotating Kerr-like black hole and probe how the LV parameter l affects the energy

flux, the conversion efficiency, the radiation temperature and the spectra of the disk in this background. In the steady-state accretion disk models, the accreting matter in the disk can be described by an anisotropic fluid with the energy-momentum tensor [19, 20]

$$T^{\mu\nu} = \varepsilon_0 u^\mu u^\nu + 2u^{(\mu} q^{\nu)} + t^{\mu\nu}, \quad (24)$$

where the quantities ε_0 , q^μ and $t^{\mu\nu}$ denotes the rest mass density, the energy flow vector and the stress tensor of the accreting matter, respectively, which are defined in the averaged rest-frame of the orbiting particle with four-velocity u^μ . In the averaged rest-frame, we have $u_\mu q^\mu = 0$ and $u_\mu t^{\mu\nu} = 0$ since both q^μ and $t^{\mu\nu}$ is orthogonal to u^μ [19, 20].

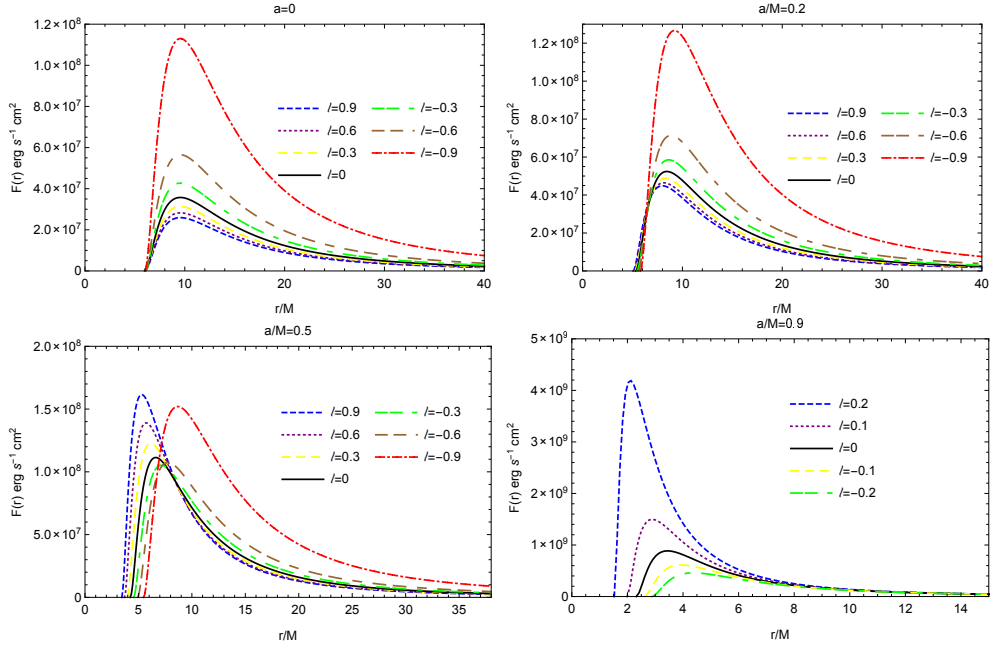


FIG. 2: The energy flux $F(r)$ with the LV parameter l in the thin disk around the rotating Kerr-like black hole. Here, we set the total mass of the black hole $M = 10^6 M_\odot$ and the mass accretion rate $\dot{M}_0 = 10^{-12} M_\odot \text{ yr}^{-1}$.

In background of the rotating Kerr-like black hole, one can find that the time-averaged radial structure equations of the thin disk can be expressed as

$$\dot{M}_0 = -2\pi\sqrt{-G}\Sigma(r)u^r = \text{Const}, \quad (25)$$

$$\left[\dot{M}_0 \tilde{E} - 2\pi\sqrt{-G}\Omega W_\phi^r \right]_{,r} = 2\pi\sqrt{-G}F(r)\tilde{E}, \quad (26)$$

$$\left[\dot{M}_0 \tilde{L} - 2\pi\sqrt{-G}W_\phi^r \right]_{,r} = 2\pi\sqrt{-G}F(r)\tilde{L}, \quad (27)$$

with

$$\Sigma(r) = \int_{-H}^H \langle \varepsilon_0 \rangle dz, \quad W_\phi^r = \int_{-H}^H \langle t_\phi^r \rangle dz, \quad \sqrt{-G} = \sqrt{1+lr}, \quad (28)$$

where $\Sigma(r)$ and W_ϕ^r are the averaged rest mass density and the averaged torque, respectively. The quantity $\langle t_\phi^r \rangle$ is the average value of the $\phi - r$ component of the stress tensor over a characteristic time scale Δt and the azimuthal angle $\Delta\phi = 2\pi$. With the energy-angular momentum relation for circular geodesic orbits $\tilde{E}_{,r} = \Omega \tilde{L}_{,r}$, one can eliminate W_ϕ^r from Eqs.(26) and (27), and then obtain the expression of the energy flux in the mass accretion process

$$F(r) = -\frac{\dot{M}_0}{4\pi\sqrt{-G}} \frac{\Omega_{,r}}{(\tilde{E} - \Omega\tilde{L})^2} \int_{r_{ms}}^r (\tilde{E} - \Omega\tilde{L})\tilde{L}_{,r} dr. \quad (29)$$

Here, we consider the mass accretion driven by black holes with a total mass of $M = 10^6 M_\odot$, and with a mass accretion rate of $\dot{M}_0 = 10^{-12} M_\odot \text{ yr}^{-1}$ [24]. In Fig. (2), we plot the total energy flux $F(r)$ radiated by a thin disk around the Kerr-like black hole for the LV parameter l and rotation parameter a . As particles is around the Schwarzschild-like black hole ($a = 0$), the energy flux $F(r)$ originates from the same value and then decreases with of the LV parameter l . However, the position of the peak value of $F(r)$ is at the same place of r . The main mathematical reason is that the marginally stable orbit radius r_{ms} , the specific energy \tilde{E} , the specific angular momentum \tilde{L} and the angular velocity Ω of the particle moving in circular orbit on the equatorial plane in the Schwarzschild-like black hole have no changes compared with the Schwarzschild case. As the rotation parameter a increases from 0 to M . the increase of the energy flux $F(r)$ with the positive LV parameter l is larger than that decrease of the energy flux $F(r)$ with the negative LV parameter l . Thus, for the rapidly rotating Kerr-like black hole, the energy flux $F(r)$ increases with l .

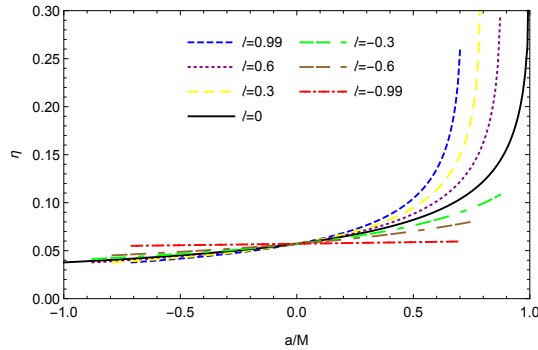


FIG. 3: The efficient η with the parameter l for the thin disk around the rotating Kerr-like black hole.

In the mass accretion process around a black hole, the conversion efficiency is an important characteristic quantity which describes the capability of the central object converting rest mass into outgoing radiation. In general, the conversion efficiency can be given by the ratio of two rates measured at infinity [18, 19]: the rate of the radiation energy of photons escaping from the disk surface to infinity and the mass-energy transfer rate

of the central compact object in the mass accretion. If all the emitted photons can escape to infinity, one can find that the efficiency η is determined by the specific energy of a particle at the marginally stable orbit r_{ms} [20]

$$\eta = 1 - \tilde{E}_{ms}. \quad (30)$$

The dependence of the conversion efficiency η on the LV parameter l is plotted in Fig.(3). It shows that the η increases with l in the prograde orbit ($a > 0$), and decreases with l in the retrograde orbit ($a < 0$). This means that the conversion efficiency of the thin accretion disk in the Kerr-like black hole with the larger positive l is more higher than that the Kerr case.

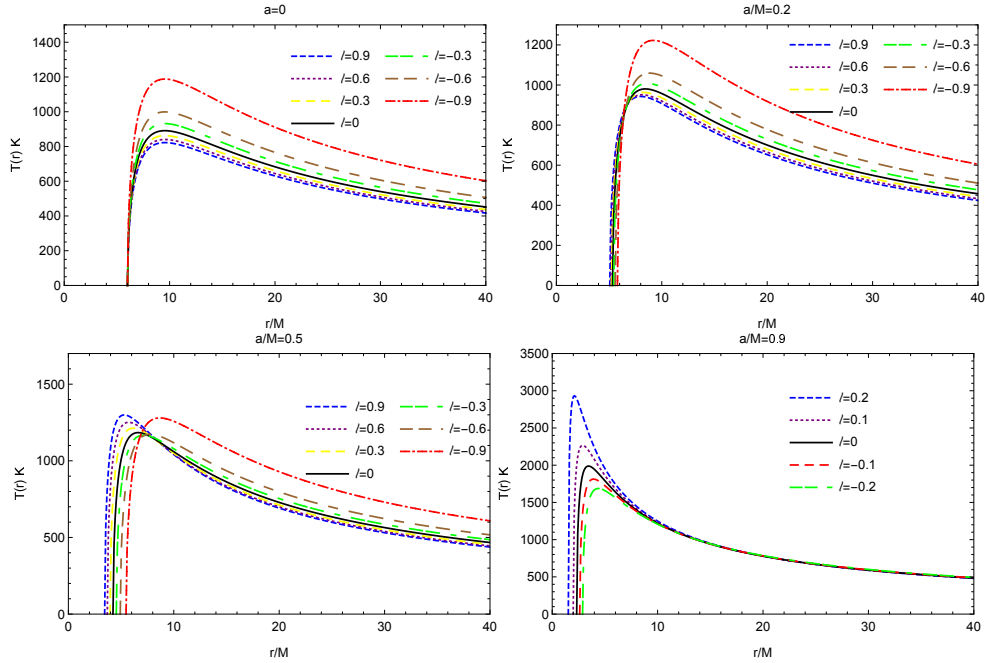


FIG. 4: The temperature T with the LV parameter l in the thin disk around the rotating Kerr-like black hole. Here, we set the total mass of the black hole $M = 10^6 M_\odot$ and the mass accretion rate $\dot{M}_0 = 10^{-12} M_\odot \text{ yr}^{-1}$.

Let us now to probe the effects of l on the radiation temperature and the spectra of the disk around the rotating Kerr-like black hole. In the steady-state thin disk model [19, 20], it is assumed generally that the accreting matter is in thermodynamic equilibrium, which means that the radiation emitted by the disk surface can be considered as a perfect black body radiation. The radiation temperature $T(r)$ of the disk is related to the energy flux $F(r)$ through the expression $T(r) = [F(r)/\sigma]^{1/4}$, where σ is the Stefan-Boltzmann constant. This means that the dependence of $T(r)$ on l is similar to that of the energy flux $F(r)$ on l , which is also shown in Fig.(4). Repeating the operations in [27], one can find that the observed luminosity $L(\nu)$ for the

thin accretion disk around the rotating Kerr-like black hole can be expressed as

$$L(\nu) = 4\pi d^2 I(\nu) = \frac{8\pi h \cos \gamma}{c^2} \int_{r_i}^{r_f} \int_0^{2\pi} \frac{\nu_e^3 \sqrt{-G} dr d\phi}{e^{h\nu_e/KT(r)} - 1}, \quad (31)$$

The emitted frequency is given by $\nu_e = \nu(1+z)$, where the redshift factor can be written as

$$1+z = \frac{1 + \Omega r \sin \phi \sin \gamma}{\sqrt{-g_{tt} - 2\Omega g_{t\phi} - \Omega^2 g_{\phi\phi}}}, \quad (32)$$

where we have neglected the effect of light bending [21, 23, 25]. The quantity d is the distance to the source,

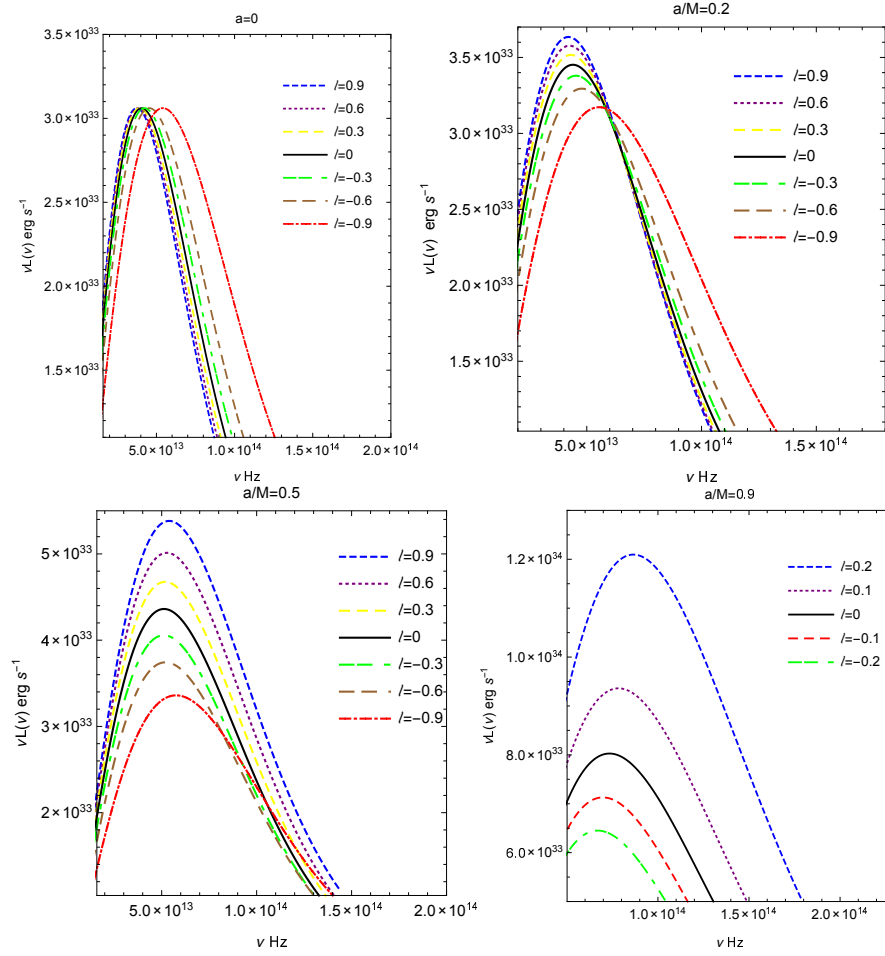


FIG. 5: The emission spectrum with the LV parameter l in the thin disk around the rotating Kerr-like black hole. Here, we set the total mass of the black hole $M = 10^6 M_\odot$, the mass accretion rate $\dot{M}_0 = 10^{-12} M_\odot \text{ yr}^{-1}$ and the disk inclination angle $\gamma = 0^\circ$.

$I(\nu)$ is the thermal energy flux radiated by the disk, and γ is the disk inclination angle. The quantities r_f and r_i are the outer and inner border of the disk, respectively. In order to calculate the luminosity $L(\nu)$ of the disk, we choose $r_i = r_{ms}$ and $r_f \rightarrow \infty$ since the flux over the disk surface vanishes at $r_f \rightarrow \infty$ in the rotating Kerr-like black hole spacetime. Resorting to numerical method, we calculate the integral (31) and present the spectral energy distribution of the disk radiation in Fig.(5). As particles is around the Schwarzschild-like

black hole ($a = 0$), the smaller value of l only leads to the higher cut-off frequencies, and the peak value of observed luminosity has no changes and is independent of l . The main mathematical reason is the same as the case of energy flux $f(r)$. As the rotation parameter a increases from 0 to M , the increase of both the cut-off frequencies and observed luminosity with the positive LV parameter l is larger than that decrease of both the cut-off frequencies and observed luminosity with the negative LV parameter l . Thus, for the rapidly rotating Kerr-like black hole, both the cut-off frequencies and observed luminosity increase with l . Moreover, we also find that the effect of the LV parameter l on the spectra becomes more distinct for the rapidly rotating Kerr-like black hole.

IV. SUMMARY

In summary, we have studied the properties of the thin accretion disk around the rotating Kerr-like black hole in Einstein-bumblebee gravity model. we have carried out an analysis of the marginally stable orbit radius r_{ms} . We have also presented the conversion efficiency η of the accreting mass into radiation, and we have showed that the Kerr-like black hole with the positive parameter l are much more efficient in converting the accreting mass into radiation than their Kerr black holes counterparts. Our results show that the LV parameter l imprints in the energy flux, temperature distribution and emission spectra of the disk. For the Schwarzschild-like black hole ($a = 0$), the larger LV parameter l diminishes the energy flux, the radiation temperature, and cut-off frequency of the thin accretion disk. the peak value of both the observed luminosity and conversion efficiency is independent of l . The main mathematical reason is that the marginally stable orbit radius r_{ms} , the specific energy \tilde{E} , the specific angular momentum \tilde{L} and the angular velocity Ω of the particle moving in circular orbit on the equatorial plane in the Schwarzschild-like black hole have no changes compared with the Schwarzschild case. As the rotation parameter a increases from 0 to $0.9M$, the larger(smaller) LV parameter l increases(diminishes) more distinct the energy flux, the radiation temperature, the observed luminosity and cut-off frequency of the thin accretion disk. Since the energy flux, the temperature distribution of the disk, the spectrum of the emitted black body radiation, as well as the conversion efficiency show, Kerr-like black hole in Einstein-bumblebee gravity model, significant differences as compared to the general relativistic case, the determination of these observational quantities could discriminate, at least in principle, between standard general relativity and Einstein-bumblebee gravity.

V. ACKNOWLEDGMENTS

Changqing's work was supported by NNSFC No.11447168, the Natural Science Foundation of of Hunan University of Humanities Science and Technology No. 2016PY06, the State Scholarship Fund of China No. 201708430087. Chikun's work was supported by the National Natural Science Foundation of China under Grant Nos.11247013; Hunan Provincial Natural Science Foundation of China under Grant Nos. 12JJ4007 and 2015JJ2085. J. Jing's work was partially supported by the National Natural Science Foundation of China under Grant No.10935013; 973 Program Grant No. 2010CB833004.

-
- [1] V. A. Kostelecký and S. Samuel, Phys. Rev. D **39**, 683 (1989).
 - [2] V. A. Kostelecky and R. Potting, Nucl. Phys. B **359**, 545 (1991); Phys. Lett. B **381**, 89 (1996).
 - [3] S. M. Carroll, J. A. Harvey, V. A. Kostelecky, C. D. Lane and T. Okamoto, Phys. Rev. Lett. **87**, 141601 (2001).
 - [4] R. Gambini, J. Pullin, Phys. Rev. D **59**, 124021 (1999).
 - [5] W.-M. Dai, Z.-K. Guo, R.-G. Cai and Y.-Z. Zhang, Eur. Phys. J. C **77**, 386 (2017).
 - [6] D. Colladay and V.A. Kostelecký, Phys. Rev. D **55**, 6760 (1997); Phys. Rev. D **58**, 116002 (1998); V. A. Kostelecký, Phys. Rev. D **69**, 105009 (2004).
 - [7] S. R. Coleman and S. L. Glashow, Phys. Lett. B **405**, 249 (1997); Phys. Rev. D **59**, 116008 (1999); R. C. Myers and M. Pospelov, Phys. Rev. Lett. **90**, 211601 (2003).
 - [8] G. Rubtsov, P. Satunin and, S. Sibiryakov, J. Cosmo. Astro. Phys. (JCAP) **05**, 049(2017).
 - [9] A. Övgün, K. Jusufi and I. Sakalli, Phys. Rev. D **99**, 024042 (2019).
 - [10] R. Casana, A. Cavalcante, F. P. Poulis, and E. B. Santos, Phys. Rev. **D97**, 104001 (2018).
 - [11] D. Capelo and J. Paramos, Phys. Rev. D **91**, 104007 (2015).
 - [12] W. D. R. Jesus and A. F. Santos, Modern Physics Letters A **34**, No. 22, 1950171 (2019)
 - [13] A. F. Santos, A. Yu. Petrov, W. D. R. Jesus, and J. R. Nascimento, Mod. Phys. Lett. A **30**, 1550011 (2015).
 - [14] C. A. Hernaski, Phys. Rev. D **90**, 124036 (2014).
 - [15] R. V. Maluf, J. E. G. Silva, and C. A. S. Almeida, Phys. Lett. B **749**, 304 (2015).
 - [16] C. Ding, C. Liu R. Casana and A. Cavalcante, arXiv:1910.02674 [gr-qc]
 - [17] N. I. Shakura and R. A. Sunyaev, Astron. Astrophys. **24**, 33(1973).
 - [18] I. D. Novikov and K. S. Thorne, in Black Holes, ed. C. DeWitt and B. DeWitt, New York: Gordon and Breach (1973).
 - [19] D. N. Page and K. S. Thorne, Astrophys. J. **191**, 499(1974).
 - [20] K. S. Thorne, Astrophys. J. **191**, 507 (1974).
 - [21] J. P. Luminet, Astron. Astrophys. **75**, 228(1979).
 - [22] J. Gair, C. Li and I. Mandel, Phys. Rev. D **77**, 024035 (2008).
 - [23] C. Bambi and E. Barausse, Astrophys. J. **731**, 121(2011).
 - [24] T. Harko, Z. Kovacs and F. S. N. Lobo, Class. Quant. Grav. **27**, 105010(2010); Phys. Rev. D **80**, 044021(2009); Phys. Rev. D **78**, 084005(2008); Phys. Rev. D **79**, 064001 (2009); Class. Quant. Grav. **26**, 215006 (2009).

- [25] S. Bhattacharyya, A. V. Thampan and I. Bombaci, *Astron. Astrophys.* **372**, 925(2001).
- [26] Z. Kovacs, K. S. Cheng and T. Harko, *Astron. Astrophys.* **500**, 621(2009).
- [27] D. Torres, *Nucl. Phys. B* **626**, 377 (2002).
- [28] Y. F. Yuan, R. Narayan and M. J. Rees, *Astrophys. J.* **606**, 1112 (2004).
- [29] F. S. Guzman, *Phys. Rev. D* **73**, 021501 (2006).
- [30] C. S. J. Pun, Z. Kovacs and T. Harko, *Phys. Rev. D* **78**, 084015 (2008); *Phys. Rev. D* **78**, 024043 (2008).
- [31] S. Chen and J. Jing, *Phys. Lett. B* **704**, 641 (2011).
- [32] Z. Kovacs, L. Gergely and P. Biermann, *Mon. Not. Royal Astron. Soc.* **416**, 991(2011).
- [33] C. Bambi and E. Barausse, *Phys. Rev. D* **84**, 084034(2011)
- [34] S. Bhattacharyya, R. Misra and A. V. Thampan, *ApJ* **550**, 841(2001).